Journal of The Electrochemical Society, **157** (12) D614-D619 (2010)
0013-4651/2010/157(12)/D614/6/$28.00 © The Electrochemical Society

Polyimide Surface Treatment by Atmospheric Pressure Plasma for Metal Adhesion

J. B. Park,[a] J. S. Oh,[b] E. L. Gil,[b] S. J. Kyoung,[b] J. T. Lim,[b] and G. Y. Yeom[a,b,z]

[a]*Sungkyunkwan University Advanced Institute of Nano Technology and* [b]*Department of Advanced Materials Engineering, Sungkyunkwan University, Suwon, Kyunggi-do 440-746, South Korea*

The surface of polyimide (PI) films before/after plasma surface treatment using a remote-type modified dielectric barrier discharge was investigated to improve the adhesion between the PI substrate and the metal thin film. Among the plasma treatments of the PI substrate surface using various gas mixtures, the surface treated with the $N_2/He/SF_6/O_2$ plasma showed the lowest contact angle value due to the high C═O bondings formed on the PI surface, while that treated with $N_2/He/SF_6$ showed the highest contact angle value due to the high $C–F_x$ chemical bondings on the PI surface. Specifically, when the O_2 gas flow was varied from 0 to 2.0 slm in the N_2(40 slm)/He(1 slm)/SF_6(1.2 slm)/O_2 (x slm) gas composition, the lowest contact angle value of about 9.3° was obtained at an O_2 gas flow of 0.9 slm. And it was due to the high content of oxygen radicals in the plasma, which leads to the formation of the highest C═O bondings on the PI surface. When the interfacial adhesion strength between the Ag film and PI substrate was measured after the treatment with N_2(40 slm)/He(1 slm)/SF_6(1.2 slm)/O_2(0.9 slm) followed by the deposition of Ag, a peel strength of 111 gf/mm was observed, which is close to the adhesion strength between a metal and the PI treated by a low pressure plasma.
 [DOI: 10.1149/1.3493585]

Manuscript submitted May 7, 2010; revised manuscript received August 30, 2010. Published October 14, 2010.

Recently, flexible electronic devices have been extensively studied because of their great potential in various applications, such as plastic flexible displays, electronic skins, flexible solar cells, and disposable printed electronics devices. In this context, inkjet printing technology is emerging as one of the important process technologies for electronics because it can significantly reduce the manufacturing process cost, materials waste, and number of process steps. By making use of inkjet technology, the printing of precise amounts of various materials with electrical, optical, and chemical functionalities can be achieved.[1-8] Specifically, many researchers investigating the inkjet-printed process have focused their attention on the printing of conductive films on a polymer film.

Poly [(N, N′-oxydiphenylene) pyromellitimide] polyimide (PI) film, having the structure shown in Fig. 1,[9] is one of the representative high-performance polymer films that has been widely used as the substrate in the microelectronic and flexible electronics industries because PI has the desirable properties of high temperature resistance, good mechanical strength, and good dimensional stability.[10,11] Because of these outstanding advantages, PI film is the main material used for flexible printed circuit boards, which are used in many electronic products, such as cellular phones, camera, computers, and their peripherals. However, in spite of its extensive usage and detailed characterization, the poor adhesion of metals to PI, which is a consequence of its low specific surface energy, has to be overcome to render the fabricated devices flexible and reliable. The general polyimide–metal composites have limited adhesion strength, which is a key issue to be resolved currently. So many researchers have studied the surface modification of PIs for the purpose of improving their adhesion to metals.[12-15]

Many kinds of surface modification techniques, such as wet-chemical treatment,[16] low pressure plasma treatment,[17-20] UV excimer irradiation,[21] and pulse ion irradiation[22] have been applied to PI substrates to enhance their adhesion to metals. Among the various surface modification techniques, low pressure plasma treatment processes are widely applied in the surface modification field because they have proven to be an effective technique for polymer surface modification. For this purpose, plasma surface treatment is widely used to improve the adhesion of metals to polymers through physical and chemical surface modifications. However, these days, the search is on for simple and low cost surface modification processes since the established surface treatment processes, such as low pressure plasma treatment, pulse ion radiation, etc., require high vacuum equipment, which results in complex steps in addition to low productivity.

Atmospheric-pressure plasmas have been investigated as a possible replacement for low pressure plasmas (for low pressure plasma processing, the pressure ranges from a few mTorr to a few Torr, in general) in a number of areas, including semiconductor and flat panel display processing. Also, this technique has been investigated for surface treatment, etching, and thin film deposition, due to its various advantages compared with low pressure plasma processes, such as a low cost of ownership, easier in-line application, possible higher throughput, etc.[23-26] In addition, nonthermal atmospheric pressure plasmas usually have temperatures in the range of 50–200°C, so they can be easily applied to plastic or polymer modification. Also, because of nonthermal process characteristics of the atmospheric pressure plasmas, many researchers are working on the treatment of various surfaces for the biomedical applications.[27-29]

In this study, we used an efficient atmospheric-pressure plasma in the field of surface modification to enhance the adhesion of PI to metal. Previously, various researchers investigated the modification of the polymer surfaces using atmospheric pressure plasmas. Park et al. investigated the treatment of the PI surface using Ar/O_2 atmospheric discharges, Stevens et al. treated the polymer surface using N_2/Ar/He atmospheric discharges, and Massines et al. also enhanced the polymer adhesion by using a He atmospheric discharge.[30-32] However, in this study, to produce a high density atmospheric-pressure plasma for enhanced process throughout, a modified dielectric barrier discharge called a "remote-type pin-to-plate dielectric barrier discharge (DBD)" was utilized. When a mutipin-type electrode (modified pin-to-plate DBD) instead of a blank electrode (conventional DBD) was used as the power electrode during the operation of DBD, lower discharge voltage, higher discharge current, and higher power consumption at a give discharge voltage was obtained from previous research, and which is believed to indicate higher plasma density for the modified pin-to-plate DBD compared to those obtained by a conventional DBD. In addition, by the use of modified pin-to-plate DBD, due to the lower voltage operation compared to conventional DBD, the discharge transition to arc or filamentary discharge was prevented.[33,34] And various gases (SF_6, He, N_2, O_2) were used for the investigation of the surface treatment effect.

Experimental

Figure 2 shows a schematic diagram of the remote plasma-type pin-to-plate DBD system used in the experiment. The discharge source was composed of a multi-pin power electrode and a blank

[z] E-mail: gyyeom@skku.edu

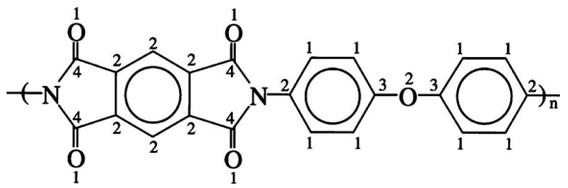

Figure 1. Schematic drawing of the polymeric unit of PMDA-ODA polyimide used in this experiment.

ground electrode located vertically above the substrate. The electrodes were made of aluminum, the size of each electrode was 50 $\times$ 300 mm^2, and both electrodes (power and ground) were coated with alumina. The discharge gap, which is the distance between the power electrode and the ground electrode, was fixed at 1 mm. The power electrode was connected to a pulse power supply with a frequency of 60 kHz and a maximum power of 10 kW, and the duty ratio was fixed at 50%. In this study, the input power was varied from 1.5 to 2.5 kW. (The operation of high power tends to cause arcing and a protection method of the source and the power supply is required. The power supply we are using for the experiment was equipped with a short circuit protector which detects an arcing condition and shuts down the power supply.) A mixture of N_2 (40 slm) and He (1 slm) was used as the charge gas, while SF_6 and O_2 were used as the reactive gases. The polyimide film (SKC KOLON PI, Gyeonnggi-do, Korea), which has the PDMA-ODA structure and was 50 μm in thickness and 100 $\times$ 100 mm^2 in size, was used in this study. The PI film was located on the 2 mm thick quartz substrate holder, and the PI film moved with the substrate holder at a constant speed under the DBD source. The polyimide substrate on the quartz substrate holder was fed below the remote-type DBD source, moving at speeds in the range from 0.25 to 1 m/min. All processes were carried out at room temperature and the distance between the substrate and the remote-type DBD source module was maintained at 4 mm.

The contact angle between the PI film and deionized water was measured using a contact angle analyzer (SEO, Phoenix 450, Gyeonnggi-do, Korea), and the optical emission intensities of the species emitted from the plasma were observed with an optical emission spectroscope [(OES) PCM 420 SC-Technology, Gyeonnggi-do, Korea] to detect radicals or activated species in the plasma. The discharge currents were measured with a current meter (PEARSON Electronix 6600, Gyeonnggi-do, Korea) and these electrical data were recorded on an oscilloscope (Tektronix TDS 340A, Gyeonnggi-do, Korea). The chemical information on the treated PI film surface was obtained using X-ray photoelectron spectroscopy [(XPS) Thermo VG SIGMA PROBE, Gyeonnggi-do, Korea]. The adhesion strength of the Ag film on the PI substrate after the atmospheric pressure plasma treatment was measured using a peel adhesion strength tester (BMSTP 50T, Gyeonnggi-do, Korea).

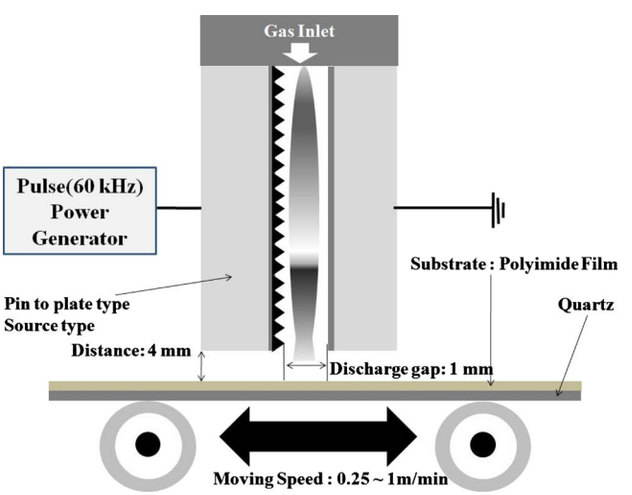

Figure 2. (Color online) Schematic diagram of the remote-type atmospheric pressure discharge system (pin-to-plate DBD) used in the experiment.

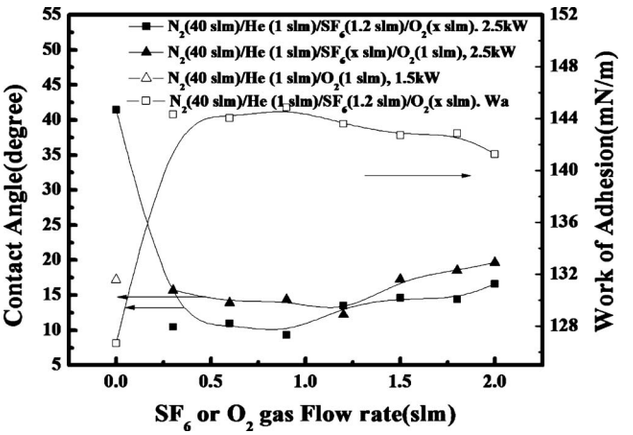

Figure 3. Contact angle measured as a function of SF_6 gas flow rate in the gas mixture of N_2(40 slm) He(1 slm)/SF_6(x slm)/O2(1 slm) and O_2 flow rate in the gas mixture of N_2(40 slm) He(1 slm)/SF_6(1.2 slm)/O_2(x slm) at a pulse power of 2.5 kW at 60 kHz. For N_2(40 slm) He(1 slm)/O_2(1 slm), a pulse power of 1.5 kW was used. For the gas mixture of N_2(40 slm) He(1 slm)/SF_6(1.2 slm)/O_2(x slm), the work of adhesion is also shown. The substrate was scanned at a speed of 0.25 m/min.

Results and Discussion

Figure 3 shows the effect of the SF_6 gas flow rate in the gas mixture of N_2(40 slm) He(1 slm)/SF_6(x slm)/O_2(1 slm) and O_2 flow rate in the gas mixture of N_2(40 slm) He(1 slm)/SF_6(1.2 slm)/O_2(x slm) on the contact angle. N_2 and He were used to maintain the glow discharge, while SF_6 and O_2 were used as the reactive gases. The PI substrate was fed below the remote-type DBD source and the scan speed of the substrate was maintained at 0.25 m/min. The pulse power to the remote-type DBD source was maintained at 2.5 kW. As shown in Fig. 3, when the O_2 flow rate was varied in the gas mixture of N_2(40 slm)/He(1 slm)/SF_6(1.2 slm)/O_2(x slm), the contact angle of the plasma treated PI film decreased significantly from 46.3° to 9.3° as the flow rate of O_2 was increased from 0 to 0.9 slm; however, further increasing the O_2 flow rate to 2 slm increased the contact angle to 16.6°. The contact angle of the as-received PI film was 41.5°. Therefore, when the PI substrate was treated with N_2(40 slm)/He(1 slm)/SF_6(1.2 slm), the contact angle was higher than that of the as-received PI film. When the SF_6 flow rate was varied from 0.3 to 2.0 slm in the gas mixture of N_2(40 slm) He(1 slm)/SF_6(x slm)/O_2(1 slm), the contact angle of the treated PI film decreased from about 11.5 to 10.0° upon the addition of 1.2 slm of SF_6, but further increasing the SF_6 flow rate to 2 slm increased the contact angle to 12.5°. Therefore, no significant change in the contact angle was observed, even though the lowest value was obtained at an SF_6 flow rate of 1.2 slm. When the discharge was operated with N_2(40 slm) He(1 slm)/O_2(1 slm), it was unstable and showed a transition from a glow discharge to a filamentary discharge with arcing during the operation of the remote-type DBD source above 1.5 kW and, therefore, a lower pulse power of 1.5 kW, rather than 2.5 kW, was used for the treatment of the PI substrate for the gas mixture of N_2(40 slm) He(1 slm)/O_2(1 slm).

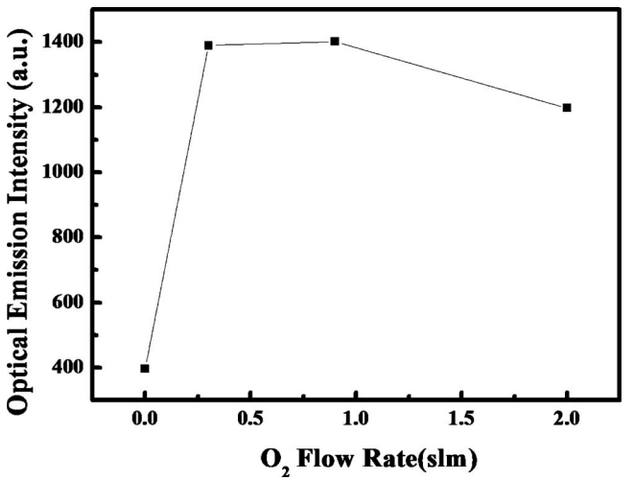

Figure 4. Discharge current measured as a function of the input power with the gas mixtures of N_2(40 slm)/He(1 slm)/O_2(0.9 slm), N_2(40 slm)/He(1 slm)/SF_6(1.2 slm), and N_2(40 slm)/He(1 slm)/O_2(0.9 slm)/SF_6(1.2 slm). The input power was varied from 1.5 to 2.5 kW and the frequency was 60 kHz. For N_2(40 slm)/He(1 slm)/O_2(0.9 slm), only the discharge current at 1.5 kW is shown due to the difficulty in the operation at higher powers.

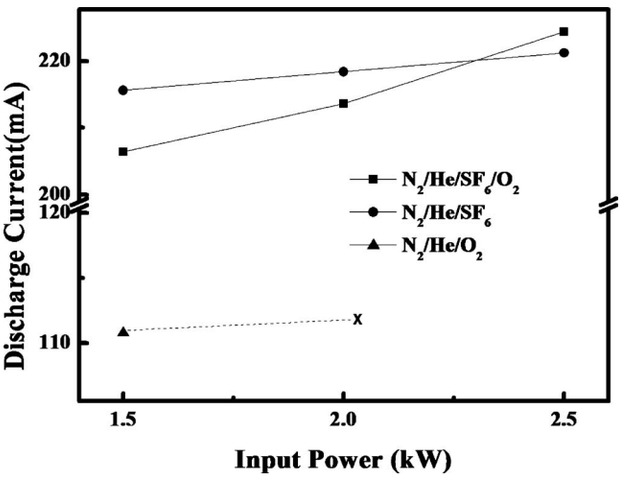

Figure 5. Optical emission intensities of oxygen atomic peak measured as a function of O_2 flow rate. The input power was maintained at 2.5 kW and the frequency was 60 kHz.

In Fig. 3, the work of adhesion is shown for the PI film treated with N_2(40 slm) He(1 slm)/SF_6(1.2 slm)/O_2(x slm) as a function of the O_2 flow rate by calculating it using the following Young–Dupre equation[35]

$$Wa = \gamma_1(1 + \cos\theta) \quad [1]$$

where γ_1 is the surface tension between the PI film and the liquid on the PI film, θ is the contact angle value of the liquid on the PI film, and Wa is the work of adhesion. In general, the work of adhesion is inversely proportional to the contact angle and, therefore, at the lowest contact angle of 9.3° which was obtained by the treatment with N_2(40 slm)/He(1 slm)/SF_6(1.2 slm)/O_2(0.9 slm), the work of adhesion shows the highest value of 144.9 mN/m.

The improvement of the plasma characteristics with the addition of SF_6 to N_2/He/O_2 was observed by measuring the discharge current of the source with the various gas mixtures. Figure 4 shows the discharge current measured as a function of the pulse power for the gas mixtures of N_2(40 slm)/He(1 slm)/O_2(0.9 slm), N_2(40 slm)/He(1 slm)/SF_6(1.2 slm), and N_2(40 slm)/He(1 slm)/O_2(0.9 slm)/SF_6(1.2 slm). As shown in the figure, when the source was operated with N_2(40 slm)/He(1 slm)/SF_6(1.2 slm) or N_2(40 slm)/He(1 slm)/O_2(0.9 slm)/SF_6(1.2 slm), the discharge current was higher than 200 mA at a pulse power of 1.5 kW and increased with increasing power, although the increase was not very high. However, when the source was operated with N_2(40 slm)/He(1 slm)/O_2(0.9 slm), the discharge current was as low as 110 mA for a pulse power of 1.5 kW and its operation at a higher pulse power was not possible, as mentioned above. The improvement of the plasma characteristics, such as the increase in the plasma stability and plasma density, with the addition of SF_6 gas to the gas mixture of N_2(40 slm)/He(1 slm)/O_2(0.9 slm) is believed to be related to the power consumption by SF_6 gas dissociation,[36] which prevents the transition from a glow discharge to a filamentary discharge and arcing at the higher electric field, in addition to the increase in the plasma density and gas dissociation efficiency caused by the Penning ionization induced by the addition of SF_6.

The lowering of the contact angle upon the addition of SF_6 to the gas mixture of N_2(40 slm)/He(1 slm)/O_2(1.0 slm) and the increase of its flow rate up to 1.2 slm, as shown in Fig. 3, is therefore believed to be related to the improvement of the plasma properties obtained with the addition of SF_6, which increases the number of oxygen radicals in the plasma. However, the increase of the SF_6 flow rate increases the number of F radicals in the plasma, which can increase the contact angle by the formation of C–Fx on the PI surface by the reaction of the carbon in PI with the F in the plasma.[37] Therefore, the increase of the contact angle for SF_6 gas flow rates higher than 1.2 slm is believed to be related to the increase in the relative number of F radicals compared to the oxygen radicals in the plasma. The decrease of the contact angle with the addition of O_2 to N_2(40 slm)/He(1 slm)/SF_6(1.2 slm) and the increase of its flow rate up to 0.9 slm, as shown in Fig. 3, is also related to the increase in the number of oxygen radicals with increasing O_2 flow rate. However, the increase of the contact angle at O_2 flow rates higher than 0.9 slm is believed to be related to the partial transition from a glow discharge to a filamentary discharge, which decreases the plasma density and gas dissociation rate. Using an OES, the optical emission intensity of the oxygen atoms was measured at a wavelength of 844.5 nm as a function of the O_2 gas flow rate in the gas mixture of N_2(40 slm)/He(1 slm)/SF_6(1.2 slm)/O_2(x slm) and at a pulse power of 2.5 kW and the result is shown in Fig. 5. As shown in Fig. 5, the addition of O_2 at flow rates of up to 0.9 slm resulted in a high oxygen atomic optical emission intensity; however, further increasing the O_2 flow rate to 2.0 slm decreased the emission intensity, indicating that the oxygen radical density was decreased when the O_2 flow rate was higher than 0.9 slm due to the partial transition to an inefficient filamentary discharge.

The contact angle on the PI film is related to the surface energy of its surface and to the bonding states of the PI surface atoms. As shown in Fig. 1, the polymeric repeat unit of the PMDA-ODA structure for PI is composed of carbon atoms and nitrogen atoms. Therefore, to determine the bonding states of the atoms on the PI surface, XPS analysis for the carbon and nitrogen atoms on the PI substrate surface was carried out and the results are shown in Fig. 6a for C 1s and Fig. 6b for N 1s after the plasma surface treatment with various gas mixtures, viz. N_2(40 slm)/He(1 slm)/O_2(0.9 slm), N_2(40 slm)/He(1 slm)/SF_6(1.2 slm), and N_2(40 slm)/He(1 slm)/SF_6(1.2 slm)/O_2(0.9 slm). The other treatment parameters are the same as those in Fig. 3. C 1s and N 1s XPS peaks were deconvoluted into various bonding peaks as shown in the figures. For the curve fitting, a software program called AVANTAGE 3.95 (Surface Chemical Analysis), which comes with the XPS system was used. When this software is used, the binding peak fitting, therefore, the deconvolution of bonding peaks is carried out by the software after the binding peak energies are selected. The XPS C 1s spectra of both

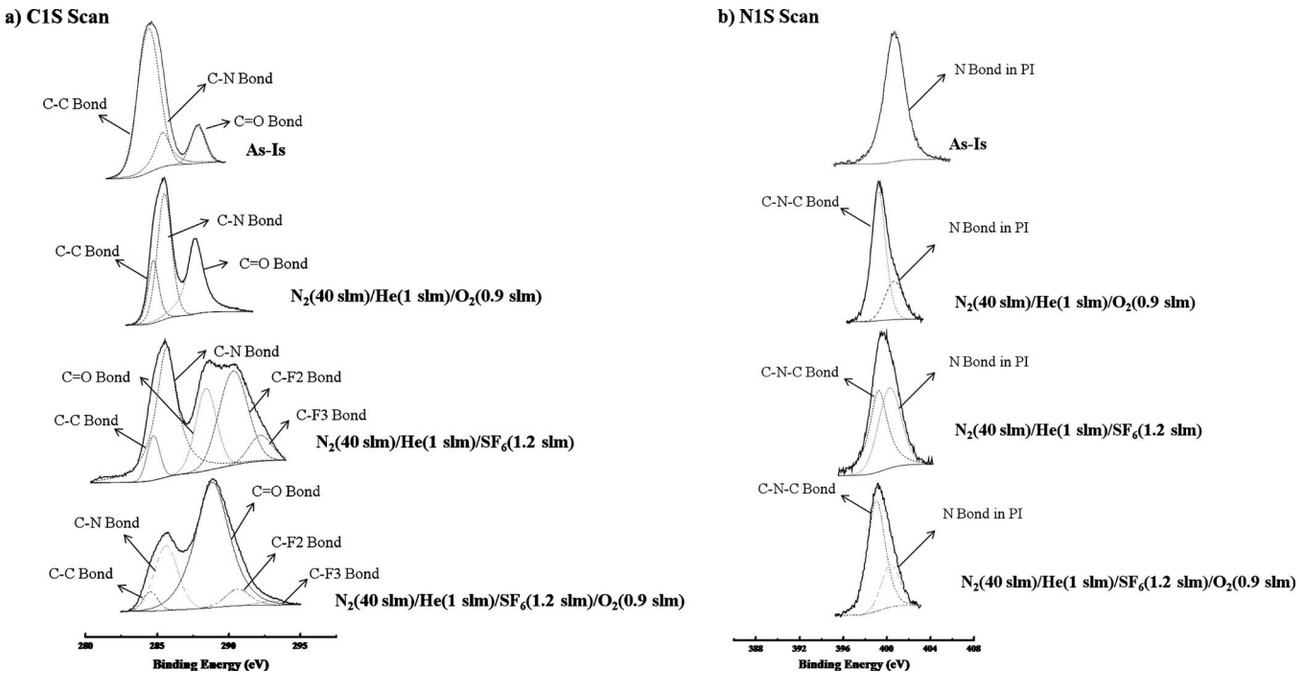

Figure 6. XPS spectra of a) C 1s peak and b) N 1s peak on the polyimide surface before/after it was treated by the atmospheric pressure plasma with N_2(40 slm)/He(1 slm)/O_2(0.9 slm), N_2(40 slm)/He(1 slm)/SF_6(1.2 slm), and N_2(40 slm)/He(1 slm)/O_2(0.9 slm)/SF_6(1.2 slm). The input power was maintained at 2.5 kW. The input power was maintained at 1.5 kW and the frequency was 60 kHz in the case of N_2(40 slm)/He(1 slm)/O_2(0.9 slm).

the nonplasma treated (as-is) and the plasma treated PI films in Fig. 6a were composed of a peak at 284.5 eV related to the C–C bonding, a peak at 285.5 eV related to the C–N bonding, and a peak at 288.6 eV related to the C═O bonding in the PMDA-ODA structure.[9,38-40] In the case of bonding peaks related to the C–C bonding and the C–N bonding, they were located so closely as shown in Fig. 6a, therefore, in some cases, it was difficult to separate those two peak intensities accurately. In addition, after the treatment by the gas mixtures containing SF_6, bonding peaks at 289.5 and 291.5 eV, which are related to C–F_2 and C–F_3, respectively, caused by the reaction of fluorine with carbon on the PI substrate surface during the plasma treatment, could be observed.[41] In the case of the XPS N 1s spectra shown in Fig. 6b, the untreated and plasma treated substrates showed a peak at 400.48 eV related to the normal N bonding (O═C–N–C═O) in the PDMA-ODA structure, while the plasma treated substrate showed an extra peak at 399.05 eV related to C–N–C bonding due to the rearrangement of the carbon atoms, oxygen atoms, and nitrogen atoms after the reaction of the ODA structure and the radicals in the plasma.[9,38]

The relative percentages of the various bonding states of the carbon and nitrogen on the PI film surface before/after the plasma treatments with different gas mixtures in Fig. 6 are shown in Fig. 7a for C 1s (C–C, C═O, C–N, C–F_2) and in Fig. 7b for N 1s (N (O═C–N–C═O), C–N–C). As shown in Fig. 7a, the percentage of C–C bonding in the untreated PI film was 72.2%, whereas it was decreased to 16.8, 6.2, and 4.2% after the plasma treatments with N_2/He/O_2, N_2/He/SF_6, and N_2/He/SF_6/O_2, respectively, due to the transition to C═O bonding or C–N bonding. The percentage of C═O bonding was increased from 12.4% for the untreated PI film to 19.1, 29.3, and 66.1% after the treatment with N_2/He/SF_6, N_2/He/O_2, and N_2/He/SF_6/O_2, respectively. Therefore, the highest percentage of C═O bonding was observed after the plasma treatment with N_2/He/SF_6/O_2. The highest percentage of C–N bonding was observed for the plasma treatment with N_2/He/O_2. In the case of the plasma treatment with the gas mixture containing SF_6, some of the C–C bonding changed to C–Fx (x = 1–3) bonding and the highest percentage of about 29.9% was observed for the treatment with N_2/He/SF_6, while the treatment with N_2/He/SF_6/O_2 resulted in a low percentage of 6.0%. In the case of N 1s, after the plasma treatment, the bonding percentage related to normal nitrogen bonding (O═C–N–C═O) in the PDMA-ODA structure was decreased from 100% to less than 50% for all of the gas mixtures and the bonding changed to C–N–C bonding.

When the bonding states after the plasma treatments of Fig. 7 are compared with the contact angles in Fig. 3, it is found that the decrease in the contact angle, which corresponds to an increase in the hydrophilic properties, is mostly related to the increase of the C═O bonding percentage on the PI film surface,[17,42] which is caused by the increase in the number of oxygen atoms transferred from the plasma to the substrate surface. On the other hand, the increase of the contact angle is related to the increase of the C–F_x bonding on the PI substrate surface for the plasma treatment with N_2/He/SF_6 which is known to increase the hydrophobic properties.[37] In the case of the plasma treatment with N_2/He/SF_6/O_2, even though the PI film contains 6.0% of C–F_x bonding, which increases the hydrophobic properties, the lowest contact angle was obtained because of the 66.1% of C═O bonding formed on the PI substrate surface, which increases the hydrophilic properties due to the increase in the number of oxygen radicals in the plasma. In fact, the surface roughness caused by surface etching or energetic particle bombardment could also affect the contact angle. However, no energetic particles can arrive at the PI substrate surface because of the remote-type DBD used in the study, where, due to the high pressure used in the experiment, the energy of the energetic particles is effectively removed by the collision with other particles before they arrive on the substrate surface. Also, the PI etch rate is extremely low when O_2 gas flow rate is lower than 1 slm, even though the PI surface is etched 1–1.5 nm/min for the O_2 gas flow rate higher than 2 slm. Moreover, for the O_2 gas flow rate in the range of 0 to 3 slm, the surface roughness remained similar at 0.6–1.3 nm. Therefore, it is believed that the change of contact angle observed in this study is related to the change of surface

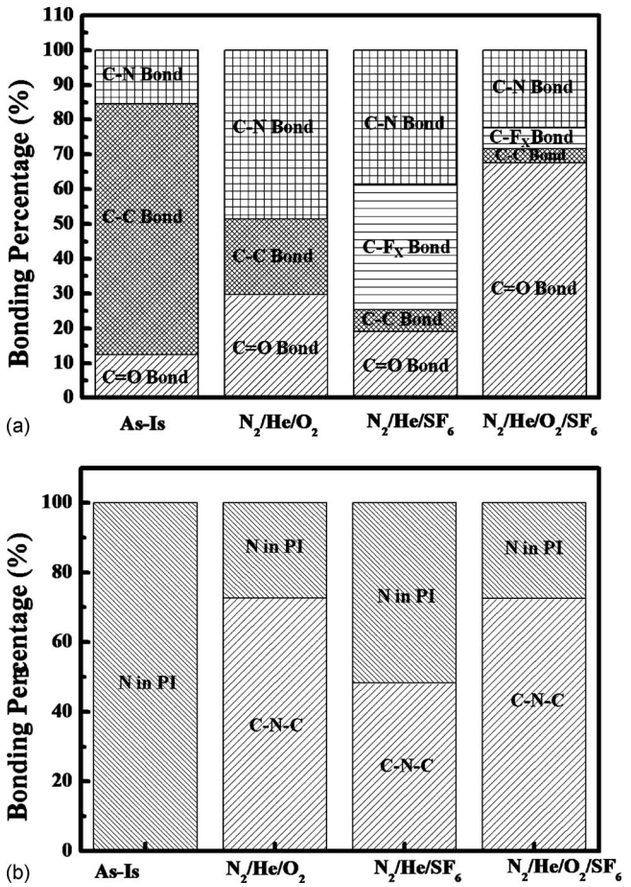

Figure 7. Chemical bonding percentages of (a) carbon and (b) nitrogen on the PI substrate before/after the plasma treatment with N_2(40 slm)/He(1 slm)/O_2(0.9 slm), N_2(40 slm)/He(1 slm)/SF_6(1.2 slm), or N_2(40 slm)/He(1 slm)/O_2(0.9 slm)/SF_6(1.2 slm). The chemical bonding percentages were obtained by the deconvolution of the XPS narrow scan data in Fig. 6.

chemistry of the PI surface rather than the change of surface roughness by energetic particle bombardment or by the etching of the PI surface.

For the plasma treatment condition of N_2(40 slm)/He(1 slm) /SF_6(1.2 slm)/O_2(0.9 slm), the moving speed of the substrate holder was varied from 0.25 to 2.0 m/min and the contact angle after the plasma treatment was measured. The results are shown in Fig. 8. The pulse power was 2.5 kW with a pulse frequency of 60 kHz. As shown in Fig. 8, the contact angle slowly increased from 9.3° at 0.25 m/min to 11° at 0.5 m/min and did not change significantly when the moving speed was further increased to 1.0 m/min. However, when the moving speed was increased to 2.0 m/min, the contact angle was also increased to 20°. Therefore, no significant change of the contact angle was observed when the substrate moving speed was increased up to 1.0 m/min. As the moving speed of the substrate holder is increased, the reaction time, which is the time between the reactive species from the plasma and PI film, is decreased. Therefore, if the treatment time is not enough by the high speed of the substrate holder, the contact angle can be affected.

To investigate the adhesion properties of a metal to the PI film, Ag was evaporated on the PI film before and after the plasma treatment and its adhesion strength was measured. The 100 nm thick Ag film was deposited at room temperature by an E-beam electron-evaporator system with the deposition rate of 7.2 nm/min. The base pressure of the E-beam evaporator before the deposition was lower than 5.0×10^{-6} Torr. To measure the adhesion force between PI

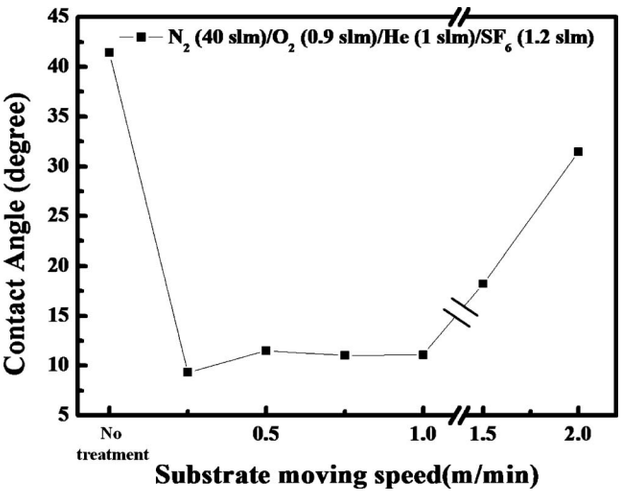

Figure 8. Contact angle measured as a function of the substrate moving speed during the plasma treatment with N_2(40 slm)/He(1 slm)/O_2(0.9 slm)/SF_6(1.2 slm). The pulse power was fixed at 2.5 kW and the frequency was 60 kHz.

film and metal (Ag 10 nm/Cu 10 μm), a 180 deg peel adhesion tester was used and the measurements were performed at the constant peeling speed of 5 mm/min, and the peeling speed was kept constant by varying the pull force. Figure 9 shows the adhesion strength of Ag evaporated on the PI film before and after the plasma treatment with N_2(40 slm)/He(1 slm)/SF_6(1.2 slm)/O_2(0.9 slm). The plasma treatment conditions are the same as those shown in Fig. 8 with a scan speed of 0.25 m/min. The thickness of Ag was 100 nm and, after the evaporation of Ag, a 10 μm thick Cu film was electroplated (required for the measurement using the peel strength tester) before the measurement of the adhesion strength using a peel strength tester. As shown in Fig. 9, after the plasma treatment, an adhesion strength of 111 gf/mm was obtained, which is more than 2 times higher than that without the plasma treatment. In previous studies, an adhesion strength of 72.6 gf/mm was reported for PI/Cr/Cu after plasma treatment at atmospheric pressure using an Ar/O_2 gas mixture[13] and an adhesion strength of 126 gf/mm for PI/Cr/Cu after low pressure plasma treatment using an O_2 gas discharge.[12] Therefore, using a modified pin-to-plate DBD, an adhe-

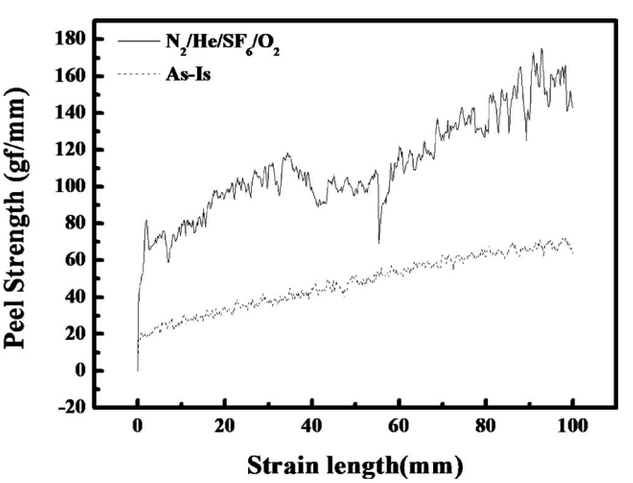

Figure 9. 180° peel strength of Ag(10 nm)/Cu(10 μm) deposited on the PI substrate measured before/after the plasma treatment of the PI substrate surface with N_2(40 slm)/He(1 slm)/O_2(0.9 slm)/SF_6(1.2 slm).

sion strength close to that obtained after the treatment by the low pressure plasma could be obtained in our experiment, even without using an adhesion promoter such as Cr between the PI film and Cu.

Conclusions

To improve the adhesion properties between the PI film and a metal thin film, the surface of the PDMA-ODA PI films was treated using a remote type modified DBD with various gas mixtures, viz. $N_2/He/SF_6$, $N_2/He/O_2$, and $N_2/He/SF_6/O_2$, and their effect on the contact angle and metal adhesion strength to the PI film was investigated.

Among the gas mixtures used in the experiment, the treatment with $N_2/He/SF_6/O_2$ resulted in the lowest contact angle value (9.3°) while $N_2/He/SF_6$ afforded a contact angle (46.3°) higher than that of the untreated film (41.5°). The high contact angle to the PI film for the plasma treatment with $N_2/He/SF_6$ was related to the formation of C–F_x bonding on the surface of the PI film, due to the reaction of carbon on the PI film surface with fluorine dissociated from SF_6. When the PI substrate surface was treated with $N_2/He/O_2$, a lower contact angle originating from the formation of C═O bondings could be obtained on the PI film surface, due to the reaction of the carbon atoms on the PI film surface with the oxygen atoms dissociated from O_2. However, due to the formation of a filamentary discharge and arcing at pulse powers higher than 1.5 kW in the case of $N_2/He/O_2$, a higher plasma density and higher oxygen dissociation could not be obtained with this plasma. A higher plasma density and higher oxygen dissociation with more stable plasma properties could be obtained by adding SF_6, that is, by using $N_2/He/SF_6/O_2$. In this case, due to the higher dissociation of the oxygen atoms, a higher C═O bonding content on the treated PI film surface could be obtained in addition to a small C–F_x bonding content. In this case, even though the C–F_x bonding can increase the contact angle, due to the large amount of C═O bondings formed on the PI film surface, the lowest contact angle was observed. When the interfacial adhesion strength between the Ag film and PI film was measured after the treatment of the PI film with N_2(40 slm)/He(1 slm)/SF_6(1.2 slm)/O_2(0.9 slm) using a peel tester, a peel strength of 111 gf/mm, which is close to the adhesion strength between a metal (Cr/Cu) and the PI treated by a low pressure plasma, was observed between Ag and the PI film.

Acknowledgments

This work was carried out through the Direct Nano Patterning Project supported by the Ministry of Knowledge Economy (MKE) under the National Strategic Technology Program. This work was also supported in part by the World Class University program of National Research Foundation of Korea (Grant no. R32-2008-000-10124-0) and by the Ministry of Education, Science and Technology (2010-0015035).

Sungkyunkwan University assisted in meeting the publication costs of this article.

References

1. B. J. de Gan, P. C. Duineveld, and U. S. Schubert, *Adv. Mater.*, **16**, 203 (2004).
2. R. F. Service, *Science*, **304**, 675 (2004).
3. C. W. Sele, T. V. Werne, R. H. Friend, and H. Sirringhaus, *Adv. Mater.*, **17**, 997 (2005).
4. H. Sirringhaus and T. Shimoda, *MRS Bull.*, **28**, 802 (2003).
5. J. W. Song, J. Kim, Y. H. Yoon, B. S. Choi, J. H. Kim, and C. S. Han, *Nanotechnology*, **19**, 095702 (2008).
6. H. Dong, W. W. Carr, and J. F. Morris, *Phys. Fluids*, **18**, 072102 (2006).
7. M. H. Tsai, W. S. Hwang, H. H. Chou, and P. H. Hsieh, *Nanotechnology*, **19**, 335304 (2008).
8. J. G. Bai, K. D. Creehan, and H. A. Kuhn, *Nanotechnology*, **18**, 185701 (2007).
9. A. M. Ektessabi and S. Hakamata, *Thin Solid Films*, **377–378**, 621 (2000).
10. *Polyimide: Synthesis, Characterization and Application*, K. L. Mittal, Editor, Plenum, New York (1984).
11. *Polyimides-Fundamentals and Applications*, M. Crosh and K. Mittal, Editors, Marcel Dekker, New York (1994).
12. S. H. Kim, S. W. Na, N.-E. Lee, Y. W. Nam, and Y. H. Kim, *Surf. Coat. Technol.*, **200**, 2072 (2005).
13. S. H. Kim, S. H. Cho, N.-E. Lee, H. M. Kim, Y. W. Nam, and Y. H. Kim, *Surf. Coat. Technol.*, **193**, 101 (2005).
14. A. K. S. Ang, E. T. Kang, K. G. Neoh, K. L. Tan, C. Q. Cui, and B. T. Lim, *Polymer*, **41**, 489 (2000).
15. A. Weber, A. Dietz, R. Pockelmann, and C. P. Klages, *J. Electrochem. Soc.*, **3**, 1131 (1997).
16. K. W. Lee, S. P. Kowalczyk, and J. M. Shaw, *Langmuir*, **7**, 2450 (1991).
17. N. Inagaki, S. Tasaka, and K. Hibi, *J. Polym. Sci. Polym. Chem.*, **30**, 1425 (1992).
18. G. Rozovskis, J. Vinkevicius, and J. Jaciauskiene, *J. Adhes. Sci. Technol.*, **10**, 399 (1996).
19. Z. J. Yu, E. T. Kang, and K. G. Neoh, *Polymer*, **34**, 4137 (2002).
20. C. H. Wen, M. J. Chuang, and G. H. Hsiue, *Appl. Surf. Sci.*, **252**, 3799 (2006).
21. J. Y. Zhang, H. Esrom, U. Kogelschartz, and G. Eming, *J. Adhes. Sci. Technol.*, **8**, 1179 (1994).
22. M. Celina, H. Kudoh, T. J. Renk, K. T. Gillen, and R. L. Clough, *Radiat. Phys. Chem.*, **51**, 2191 (1998).
23. S. Okazaki, M. Kogoma, M. Uehara, and Y. Kimura, *J. Phys. D: Appl. Phys.*, **26**, 889 (1993).
24. T. Yokoyama, M. Kogoma, S. Kanazawa, T. Moriwaki, and S. Okazaki, *J. Phys. D: Appl. Phys.*, **23**, 374 (1990).
25. T. Yokoyama, M. Kogoma, S. Kanazawa, and S. Okazaki, *J. Phys. D: Appl. Phys.*, **23**, 1125 (1990).
26. A. Majumdar and R. Hippler, *Rev. Sci. Instrum.*, **78**, 075103 (2007).
27. M. Laroussi and X. Lu, *Appl. Phys. Lett.*, **87**, 113902 (2005).
28. A. Majumdar, K. Schröder, and R. Hippler, *J. Appl. Phys.*, **104**, 074702 (2008).
29. A. Majumdar, R. Ummanni, K. Schröder, R. Walther, and R. Hippler, *J. Appl. Phys.*, **106**, 034702 (2009).
30. S. J. Park and H. Y. Lee, *Colloid Interface Sci.*, **285**, 267 (2005).
31. M. J. Shenton, M. C. Lovell-Hoare, and G. C. Stevens, *J. Phys. D: Appl. Phys.*, **34**, 2754 (2001).
32. F. Massines and G. Gouda, *J. Phys. D: Appl. Phys.*, **31**, 3411 (1998).
33. Y. H. Lee, S. J. Kyung, C. H. Jeong, and G. Y. Yeom, *Jpn. J. Appl. Phys.*, **44**, L78 (2004).
34. Y. H. Lee and G. Y. Yeom, *J. Korean Phys. Soc.*, **47**, 74 (2005).
35. N. K. Adam, *Nature*, **180**, 809 (1957).
36. F. Massinesa, P. Ségurb, N. Gherardi, C. Khamphan, and A. Ricard, *Surf. Coat. Technol.*, **174–175**, 8 (2003).
37. A. Kotzev, A. Laschewsky, P. Adriaensens, and J. Gelan, *Macromolecules*, **35**, 1091 (2002).
38. J. E. Klemberg-Sapieha, O. M. Kuttel, L. Martinu, and M. R. Wertheimer, *J. Vac. Sci. Technol. A*, **9**, 2975 (1991).
39. A. Majumdar, G. Das, K. R. Basvani, J. Heinicke, and R. Hippler, *J. Phys. Chem. B*, **113**, 15734 (2009).
40. A. Majumdar, G. Scholz, and R. Hippler, *Surf. Coat. Technol.*, **203**, 2013 (2009).
41. J. F. Moulder, W. F. Stickle, P. E. Sobol, and K. D. Bomben, *Handbook of X-Ray Photoelectron Spectroscopy*, Perkin-Elmer, Eden Prairie, MN (1992).
42. S. Stankovich, D. A. Dikin, R. D. Piner, K. A. Kohlhaas, A. Kleinhammes, Y. Jia, Y. Wu, S. T. Nguyen, and R. S. Ruoff, *Carbon*, **45**, 1558 (2007).